Acta Biochimica Polonica

Vol. 48 No. 2/2001

495–510

QUARTERLY

Mg^{2+} ions do not induce expansion of the melted DNA region in the open complex formed by *Escherichia coli* RNA polymerase at a cognate synthetic Pa promoter. A quantitative $KMnO_4$ footprinting study

Tomasz Łoziński and Kazimierz L. Wierzchowski[½]

Institute of Biochemistry and Biophysics, Polish Academy of Sciences, Warszawa, Poland

Received: 22 May, 2001; accepted: 30 May, 2001

Key words: permanganate footprinting, thymine oxidation, open promoter complex, effect of magnesium ions, RNA polymerase

Footprinting studies of prokaryotic open transcription complexes (RP_O), based on oxidation of pyrimidine residues by $KMnO_4$ and/or OsO_4 at a single oxidant dose, have suggested that the extent of DNA melting in the transcription bubble region increases in the presence of Mg^{2+}. In this work, quantitative $KMnO_4$ footprinting in function of the oxidant dose of RP_O, using *Escherichia coli* RNA polymerase ($E\sigma^{70}$) at a fully functional synthetic promoter Pa having –35 and –10 consensus hexamers, has been used to determine individual rate constants of oxidation of Ts residues in this region at 37°C in the absence of Mg^{2+} and in the presence of 10 mM $MgCl_2$, and to evaluate therefrom the effect of Mg^{2+} on the extent of DNA melting. Population distributions of end-labeled DNA fragments corresponding to oxidized Ts were quantified and analyzed according to the single-hit kinetic model. Pseudo-first order reactivity rate constants, k_i, thus obtained demonstrated that Mg^{2+} ions bound to RP_O merely enhanced the reactivity of all 11 oxidizable thymines between the +3 and –11 promoter sites by a position-dependent factor: 3–4 for those located close to the transcription start point +1 in either DNA strand, and about 1.6 for those located more distantly therefrom. On the basis of these observations, we conclude that Mg^{2+} ions bound to RP_O at Pa do not influence the length of the melted DNA region and propose that the higher reactivity of thymines results mainly from lower local repulsive electrostatic barriers to MnO_4^- diffusion around carboxylate binding sites in the catalytic center of RP_O and promoter DNA phosphates.

This work was supported in part by the State Committee for Scientific Research (KBN, Poland) grant 6 P302 024 06 to KLW.

[½]Corresponding author: Kazimierz L. Wierzchowski, Institute of Biochemistry and Biophysics, Polish Academy of Sciences, A. Pawińskiego 5a, 02-106 Warszawa, Poland; e-mail address: klw@ibb.waw.pl

Abbreviations: BSA, bovine serum albumin; DTT, dithiothreitol; $E\sigma^{70}$ or RNAP, *Escherichia coli* RNA polymerase; **nt**, nontemplate DNA strand; **t,** template DNA strand; RP_O, open complex; T, thymine residue.

It has long been known that *Echerichia coli* RNA polymerase ($E\sigma^{70}$) in the process of RNA synthesis exhibits an absolute requirement for Mg^{2+} (or another divalent cation) [1, 2], related to the binding of metal chelates of the ribonucleoside 5′-triphosphates to the elongation site of the transcriptional complex [3] and to the involvement of Mg^{2+} in the catalysis of internucleotide phosphodiester bond formation [4–9]. More recently it has been surmised that Mg^{2+} ions participate also in enlargement of the transcription bubble [10–15]. Magnesium ions at 10 mM concentration led to a several-fold increase in the number of $KMnO_4$-oxidized pyrimidine residues in the λP_R promoter open complex within the melted region, therefore propagation of DNA strands opening from the center of the transcription bubble outwards was proposed [11]. Also backbone reactivity of the λP_R promoter template strand in the open complex toward $HO^\bullet$ radicals, generated locally in the reaction of $Fe(EDTA)^{2-}$ with H_2O_2, was found significantly enhanced by 10 mM $MgCl_2$ in the single stranded region of the template strand at positions from –4 to +1 [12]. Studies on the dependence of the rate of dissociation of the binary open complex at λP_R promoter on $MgCl_2$ concentration have suggested that this process can be accompanied by the release of about 3 Mg^{2+} ions [10]. All these findings together with the evidence on the existence in a number of DNA and RNA polymerases of two crucially important carboxylate Mg^{2+}-binding sites near the catalytic site [8], led to the proposal that 2 of the 3 Mg^{2+} ions bound specifically to the RP_{O2} form of the $E\sigma^{70}$–λP_R open complex are located near the transcription start site [12]. Unidirectional expansion of the bubble towards the transcription start point as a result of Mg^{2+} binding has also been postulated for *E. coli* RNAP–T7A1 promoter complex [13] as well as for promoter complexes formed by *Bacillus subtilis* [16] and *Thermatoga maritima* [17] RNA polymerases.

The studies concerning Mg^{2+}-induced expansion of the transcription bubble were based on comparative analyses of $KMnO_4$ footprints of open complexes obtained under selected single oxidant concentration and time of exposure (a single oxidant dose) under Mg^{2+} conditions. In most of these reports, however, neither the experimental methods used nor the data obtained were presented in sufficient detail to assure the readers that the conditions of single oxidation event per DNA molecule were rigorously controlled (single-hit footprinting). Such conditions should be fulfilled to make possible a reliable interpretation of footprints in terms of relative oxidizabilities of bases in DNA–protein complexes. Only recently it has been shown [18] how to extract these data quantitatively from footprints obtained under multiple-hit conditions in function of the oxidant dose.

We have therefore studied quantitative $KMnO_4$ footprinting as a function of the oxidant dose on the open transcription complex formed at a synthetic consensus-like *E. coli* promoter Pa by the cognate RNA polymerase, in order to determine individual reactivity rate constants for T residues within the transcription bubble region, in the absence and in the presence of 10 mM $MgCl_2$, and to evaluate on this basis the effect of Mg^{2+} ions on the extent of DNA melting. The functional, kinetic and thermodynamic properties of the open complex at this promoter [19–22] were shown to be generally similar to those of the complexes at natural promoters thus far studied [22–26]. A great advantage of the use of promoter Pa in footprinting of the open complex was the presence within the melted DNA region of as much as 14 AT base pairs. We have demonstrated that binding of Mg^{2+} ions to the open transcription complex is not accompanied by an extension of the melted DNA region. This binding merely induces a characteristic change in the oxidizability pattern of T residues within the transcription bubble: a 3–4 fold increase of reactivity rate constants

of those located close to the transcription start point and a smaller, about 1.6-fold one, in the rate constants of those lying further upstream thereof. In a separate study [27], we have also investigated quantitatively the effect of 10 mM Mg^{2+} on $KMnO_4$-oxidation of pyrimidines in double-stranded DNA, and observed a similar increase in their reactivity. Most likely all these effects are due to the shielding by Mg^{2+} ions of negatively charged groups on DNA and RNAP surfaces lowering thereby repulsive interactions with MnO_4^- anions.

MATERIALS AND METHODS

Pa promoter DNA and Eσ^{70} RNA polymerase. Promoter Pa was obtained, cloned into the pDS3 plasmid and DNA was purified as described earlier [19–21]. RNA polymerase was prepared from *E. coli* K12 according to [28, 29], using Sephacryl S300 instead of Bio-Gel. Klenow fragment of DNA polymerase I and polynucleotide kinase were from Boehringer (Mannheim), and [γ-^{32}P]ATP was from Amersham. Two DNA primers, Pr(t) and Pr(nt), complementary to the template (from –138 to –117) and non-template (from +78 to +99) DNA strand, respectively, were synthesized by the solid phase phosphoramidite method, and purified by denaturing PAGE followed by DEAE-Sephacel column chromatography and ethanol precipitation. The 5′-end of the primer was phosphorylated with a 2-fold molar excess of [γ-^{32}P]ATP by polynucleotide kinase. All other chemicals were molecular biology grade products.

Open complex formation and $KMnO_4$ footprinting. Modification of nucleotides in DNA by $KMnO_4$ oxidation as a function of the oxidant dose applied and their detection by primer extension were performed according to [30, 31]. To minimize scatter of data, we used premixes that were aliquoted into a series of reactions and volumes that could be accurately pipetted.

A buffered solution of RNA polymerase and supercoiled plasmid pDS3 carrying the investigated promoter Pa was divided into halves, to one $MgCl_2$ was added to a final concentration of 10 mM and the other supplemented appropriately with pure water; then each solution was aliquoted into 50 μl samples containing: 1 pmol of pDS3, 2 pmoles of RNA polymerase, 25 mM Tris/HCl, pH 7.0, 100 mM KCl, 0.2 mM EDTA. For formation of the open complex each sample was placed at constant time intervals in a water bath at 37°C for 15 min. Then 5 μl of a $KMnO_4$ solution (freshly diluted from 0.3 M stock) was added to obtain the desired final concentration of the oxidant (0.05, 0.1, and 0.2 mM), and the reaction mixture was incubated for precisely 3 min at 37°C. The reaction was quenched by addition of 150 μl of stop solution (containing: 2 mM EDTA, 1% of β-mercaptoethanol and 5 nmoles of marker DNA – the *Sal*I–*Hin*dIII fragment of the same plasmid). The samples were deproteinized by phenol/chloroform extraction, the water phase collected and the oxidized DNA purified using a Sephadex G50 spin column.

The samples prepared as above were subjected to quantitative analysis for the extent of oxidation of thymine residues within the transcription bubble located both in the nontemplate and template DNA strands. For this analysis the samples were divided into halves and the primer extension reaction was carried out separately for each half with the appropriately designed ^{32}P-end-labeled primer, Pr(nt) or Pr(t). Reaction conditions were optimized for each strand separately to ensure the specificity of primer's hybridization. In the case of the nontemplate strand, 35 μl of the purified DNA was mixed with 4 μl of 0.01 M NaOH containing 2 pmoles of ^{32}P-end-labeled primer and denatured at 80°C for 3 min. After cooling to 0°C it was neutralized with 8 μl of Klenow reaction buffer (containing 250 mM Tris/HCl, pH 7.2, 50 mM $MgSO_4$, 1 mM DTT and 2.5 mM of each dNTP) and hybridized by incubation at 45°C for 15 min. Then 2 units of

Klenow fragment of DNA polymerase I enzyme in 2 μl of the enzyme diluent (containing 25% glycerol, 25 mM KH_2PO_4, pH 7.0, 1 mM DTT and 50 mg/ml BSA) were added and primer extension performed at the same temperature for 10 min. The reaction was quenched by addition of 18 μl of a stop solution (containing 3 M ammonium acetate, 20 mM EDTA and 2 μg tRNA). Products of the Klenow reaction were ethanol precipitated, rinsed with 70% ethanol, dried and dissolved in 10 μl of gel loading buffer (containing 70% freshly deionized formamide, 7 M urea, 3 mM NaOH, 0.1 mM EDTA and 0.02% Bromophenol blue and Xylene cyanol). After denaturing the products at 95°C for 2 min, 3 μl of single-stranded DNA solution were resolved in duplicate on 6% polyacrylamide sequencing gels in TBE buffer (containing 0.089 M Tris/borate and 2 mM EDTA, pH 8.3). Dried gels were exposed to storage phosphor screens from Molecular Dynamics. With respect to the template strand, all the reaction conditions were the same except that neutralization, hybridization and primer extension steps were carried out at 60°C, directly after denaturation at 80°C, without the cooling step at 0°C.

Each footprinting experiment was duplicated and products of each of the two reactions resolved on 2 footprinting gels, so that on the whole 4 footprints at each oxidant concentration were obtained and analyzed, as described below.

Phosphorimager analysis and quantification of band intensities. Images of footprints were obtained with the use of a Molecular Dynamics Phosphorimager. Integrated intensities of bands (or groups of bands) and their intensity profiles along gel lanes were obtained using the "ImageQuant" software, by the volume integration and area integration options, respectively. For area integration, the lowest intensity point in the graph was used as the horizontal baseline (background). For volume integration, local background was used for bands corresponding to promoter bubble DNA fragments, whereas for the whole lanes gel without any radioactivity (outside the lanes). These data were analyzed further with software: "Origin^{TM}" from MicroCal Software and "Quattro Pro 4.0" from Borland.

The scans were analysed in three steps. First, the integrated intensity (IQvolume integration) of the group of bands corresponding to DNA fragments terminated at all oxidized bases within the transcription bubble was measured and normalized to the integrated intensity of the whole lane. Then the distribution of the integrated intensity within the bubble along the lane, an intensity profile, was obtained using the IQarea integration function. Integrated intensities of particular bands were evaluated by deconvolution of the intensity profiles assuming Gaussian distribution of the intensity within the bands and a constant halfwidth for all the bands.

RESULTS

Our main goal in this study was to determine the rate constants of oxidation by $KMnO_4$ of individual thymine residues within the melted DNA region of the open complex and evaluation on this basis of the effect of Mg^{2+} ions on the reactivity of these bases and the length of the transcription bubble. For this purpose, the open complex formed by Eσ^{70} at a strong synthetic promoter Pa, containing –10 and –35 consensus recognition hexamers and the bubble region made exclusively of AT base pairs (Fig. 1), was subjected to increasing concentrations of $KMnO_4$ at a constant exposure time (dose: x = [$KMnO_4$] × 180 s) at 37°C in the absence and presence of 10 mM $MgCl_2$ in the reaction buffer. Conditions of the oxidation reaction were chosen according to the commonly used recommendations [31], including $KMnO_4$ concentration high enough to satisfy conditions for pseudo first-order oxidation reaction with pyrimidines, a proper time of exposure to the oxidant and close to physio

logical 10 mM $MgCl_2$ concentration. Thymine residues oxidized to corresponding thymine glycols [32] were localized on both the nontemplate (**nt**) and template (**t**) DNA strands by the technique of DNA primer extension with Klenow fragment of DNA polymerase I, and appropriately designed

Figure 1. Sequence of the synthetic promoter Pa cloned into pDS3 plasmid.

Transcription start site (+1) indicated by kinked arrow, 14 AT bp long transcription bubble in bold font, arrows indicate direction of extension of end-labeled primers Pr(t) and Pr(nt) by Klenow enzyme (in brackets location relative to the start site).

ual bands were used to calculate fractions f_i of DNA fragments corresponding to particular oxidized T_i residues. Partition of DNA fragments between twin bands due to termination of the primer extension reaction both at a thymine glycol (Tg) and at a preceding base when the glycol form was hydrolyzed to urea (Tu), was accounted for in calculations of f_i's under the assumption that the ratio of the two forms f(Tg)/f(Tu) was independent of base sequence. This ratio was estimated from integrated areas of the bands seen at the edges of footprinted sequences: T(+2)T(+3)G(+4) and A(–12)T(–11) in the non-template and template strands, respectively.

5′-^{32}P-labeled DNA primers [31]. This allowed to compare directly the reactivity of the two DNA strands within the melted DNA region of the open complex. End-labeled DNA products, viz. DNA fragments terminated at individual oxidized thymine residues in a given strand within the transcription bubble, were separated on a polyacrylamide sequencing gel yielding footprints exemplified in panels (a) and (c) of Fig. 2. The integrated areas of groups of bands corresponding to oxidized bases within the bubble region, corrected for local background radioactivity and normalized to the integrated intensity of the whole lane, were deconvoluted into individual components assuming Gaussian distribution of the intensity within bands (cf. panels b and d of Fig. 2). Note that due to the termination of the primer extension reaction at a base preceding T, when the glycol form of the latter was hydrolyzed to an urea derivative during alkaline denaturation [33, 34], some oxidized Ts appear as doublets of bands while those corresponding to T_n runs were unresolved n+1 multiplets (cf. bands indicated by arrows in panels b and d of Fig. 2). Areas under individ-

Inspection of the footprints and intensity profiles shows that, at a sufficiently high oxidant dose applied, even in the absence of $MgCl_2$, the DNA bands of greatly differentiated intensity seen between the –10 and +1 promoter regions correspond to 11 thymine residues located therein: T+3, T+2, T–2, T–3, and T–4 of the **nt** strand, and T+1, T–1, T–5, T–8, T–9 and T–11 of the **t** strand. In the presence of 10 mM $MgCl_2$ all these bands appear at a lower oxidant dose. None of these bands were present in footprints obtained in the absence of RNA polymerase for intact and $KMnO_4$ oxidized DNA under similar conditions (not shown). The $KMnO_4$ reactivity of respective Ts in dsDNA form of the Pa promoter under similar salt conditions was shown elsewhere [27] to be 2–3 orders of magnitude

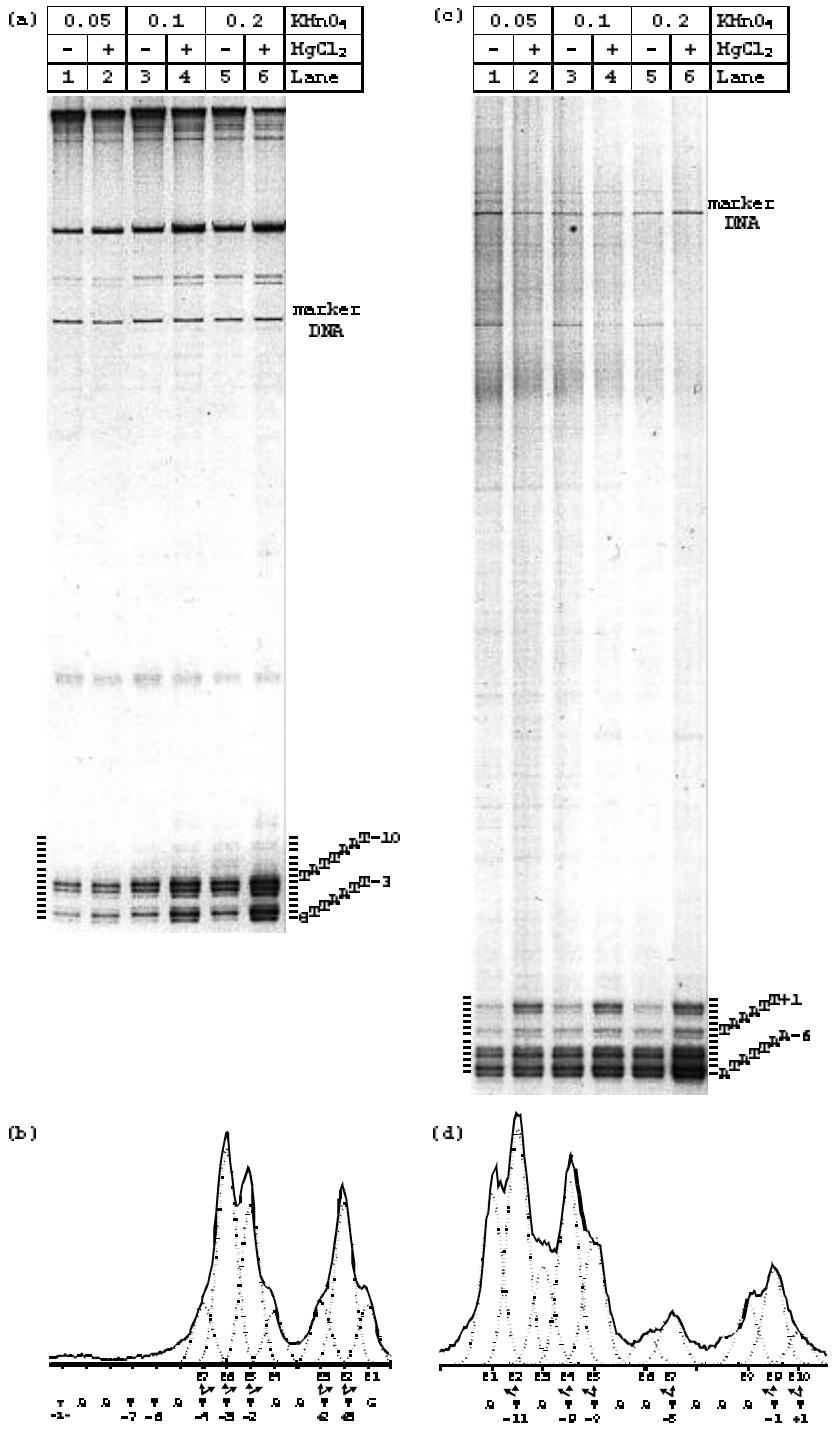

Fig ure 2. $KMnO_4$ footprinting of Eσ^{70}–Pa pro moter com plexes.

Footprinting as a func tion of $KMnO_4$ con cen tra tion in the ab sence and in the pres ence of 10 mM $MgCl_2$ was performed as de scribed in Ma te rials and Methods. Panels (a) and (c): autoradiograms of PAGE re solved ^{32}P-end-labeled DNA prod ucts of Klenow primer ex ten sion re ac tion car ried out on the nontemplate and tem plate DNA strands, respec tively; $KMnO_4$ con cen tra tions (in mM) in di cated at the top of lanes 1–6, "–" and "+" signs in di cate the absence and pres ence of 10 mM $MgCl_2$ in footprinting re ac tions; along the rightmost lanes are in di cated DNA bands cor respond ing to mark ers DNA's (329 nt and 833 nt long in (a) and (c), re spec tively) and to in di vid ual bases of Pa within the bub ble re gion. Panels (b) and (d): se lected (lanes 4) in te grated in ten sity pro files of Pa bub ble (solid lines), deconvoluted into Gaussian components P1–P10 (dotted lines) corresponding to individual oxidized thymines (marked by ar rows).

lower than that found for **nt** strand thymines: T+3, T+2, T–2, T–3 and T–4 in ssDNA form in the RP_O. Thus, it can be safely concluded that the transcription bubble region spans at least 14 bp between positions +3 and –11 of the promoter Pa.

It is apparent that while all Ts of the **t** strand within the transcription bubble did appear oxidizable, T–6, T–7 and T–10 in the –10 region of the of the **nt** strand were inaccessible to the oxidant under the single-hit regime. Faint bands due to respective DNA fragments were too weak to be quantified reliably; moreover, they came up more clearly only at higher oxidant doses (not shown) corresponding to multiple-hit reaction, accompanied by simultaneous oxidation of RNAP and severe perturbation of the open complex structure (T. Łoziński, unpublished observation).

The f_i data determined as a function of the oxidant dose (x = ct, [Ms]), plotted in Figs. 3 and 4, were subjected to kinetic analysis. The plots clearly show the strong and greatly differentiated effect of Mg^{2+} ions on the oxidizability of particular thymines within the melted DNA region.

The range of oxidant doses within which the single-hit footprinting regime could be regarded to prevail was evaluated according to the proposed criteria [18]; in most cases the upper limit was found between 0.018 and 0.036 Ms. The $f_i(x)$ data as well as fractions $f_u(x)$ of unoxidized DNA corresponding to these conditions conformed to a single exponential functions:

$$f_i = 1–\exp(–k_i\ x) \quad (1)$$

and

$$f_u = \exp(–\Sigma k_i\ x) \quad (2),$$

where x = ct is the oxidant dose, Σk_i is the pseudo-first order rate constant of oxidation of an i-th thymine, and Σk_i a sum taken over all i. At $x \geq 0.036$ Ms, f_i did not obey a pseudo-first order relationship with the oxidant dose (not shown except for x = 0.036 Ms, cf. data points falling down from the fitted curve in some panels of Figs. 3 and 4; these points were not included in fitting), i.e. the footprinting conditions corresponded to the multiple-hit oxidation regime [18].

The rate constants k_i were derived with a reasonable accuracy from the global non-linear least squares analysis of all the experimental $f_i(x)$ and $f_u(x)$ data according to equations (1) and (2). Inspection of the kinetic data column plotted in Fig. 5a shows that, in the absence of Mg^{2+} ions, values of the measured k_i vary in a characteristic way with the location of corresponding T with respect to the +1 transcription start point and greatly differ one from another by a factor up to approx. 20. Thymines located close to the transcription start point: T+1, T–1 of the **t** strand and T+2 of the **nt** strand proved to be weakly reactive. The most reactive were T–11, T–9 and T–8 of the **t** strand and T–3 of its complementary counterpart of the **nt** strand. In the presence of Mg^{2+}, the reactivity of all Ts in both strands was strongly enhanced (cf. plot of $k_{i,Mg}/k_i$ values in Fig. 5b). The largest increase in reactivity was exhibited by weakly reactive thymines, especially by T+1 and T–1 of the **t** strand by a factor of about 3.7 and 4.3, respectively, and T+3 and T+2 of the **nt** strand by a smaller factor of approx. 2.6. The reactivity of all the remaining Ts, located in either DNA strand more distantly from the transcription start point, was increased by a similar factor of approx. 1.6. Thymine residues wihin the bubble region of the Pa promoter can be thus divided into two classes of distinctly different reactivity and magnitude of Mg^{2+} effect: (i) located close to the active center of RPo and (ii) upstream therefrom.

DISCUSSION

The presented results of $KMnO_4$ footprinting of the open complex formed by $E\sigma^{70}$ holoenzyme at the cognate Pa promoter clearly demonstrate that, in the absence of

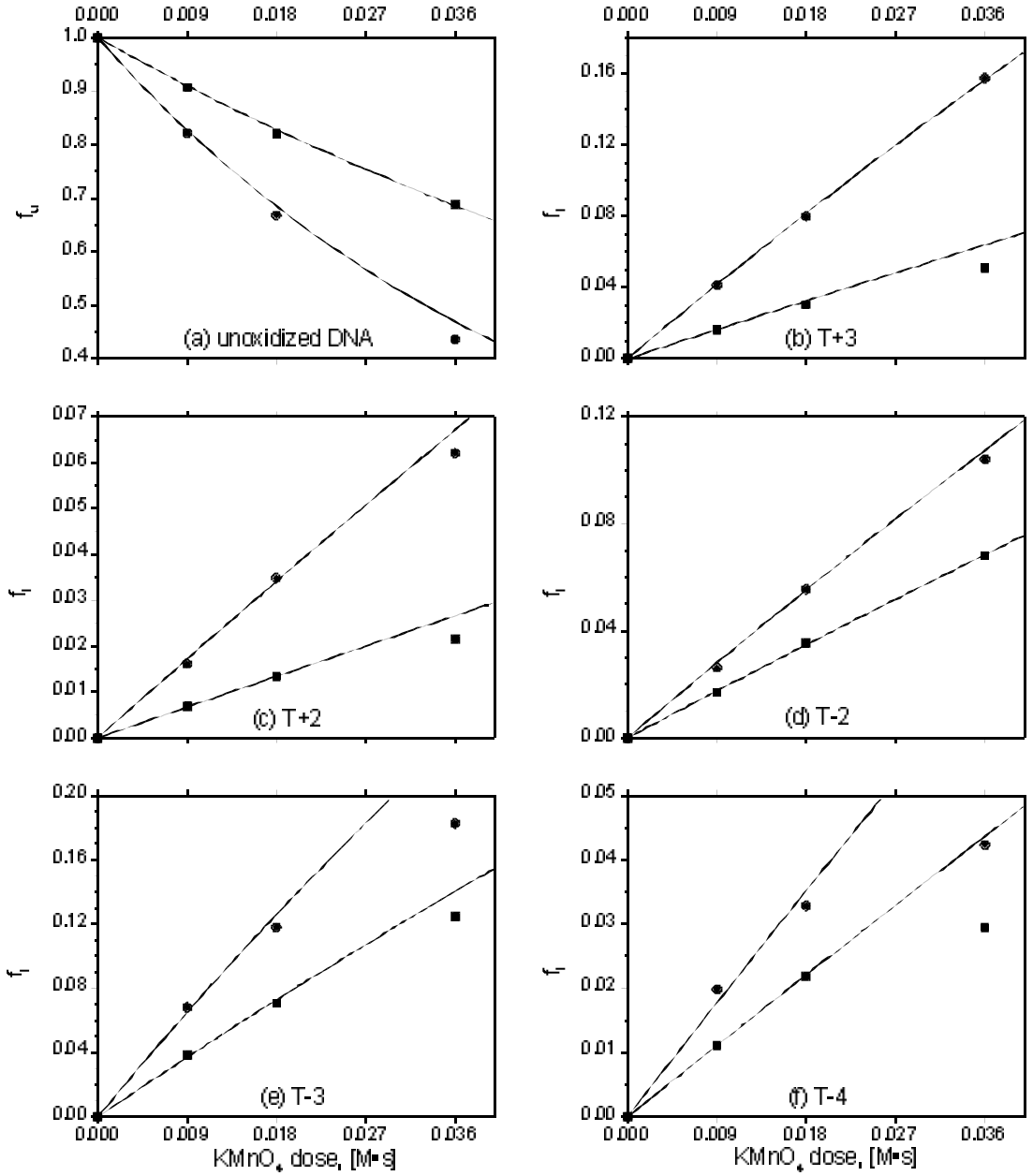

Figure 3. Kinetics of oxidation of thymines in the bubble region of the nontemplate DNA strand of the Pa promoter in the open transcription complex at 37°C.

Data points $f_i(x)$ corresponding to DNA fractions of unoxidized DNA (f_u, panel a) and oxidized thymines (f_i, marked T_i in panels b–f) at different $KMnO_4$ doses (x) in the absence (solid squares) and in the presence (solid circles) of 10 mM $MgCl_2$ were obtained by quantification of footprints (exemplified in Fig. 2, panels a and c) as described in Materials and Methods; calculated mean standard deviation (n = 4) was in the range of 5–20% relative to the $f_i(x)$ value. The solid lines correspond to fitted single-exponential functions (eqns. 1 or 2).

Mg^{2+}, the upstream end of the melted DNA domain is defined by the most reactive T–11 in the **t** strand and the downstream end thereof by T+3 in the **nt** strand. Since these two thymines are 3′-flanked by unreactive purines, the length of the transcription bubble domain is at least 14 bp long. In the presence of bound Mg^{2+} (at 10 mM $MgCl_2$), the position-dependent reactivity of all the oxidizable Ts is increased in a characteristic manner: strongly of those located in either DNA strand close to the +1 position, and uniformly to a smaller extent of those located more distantly therefrom.

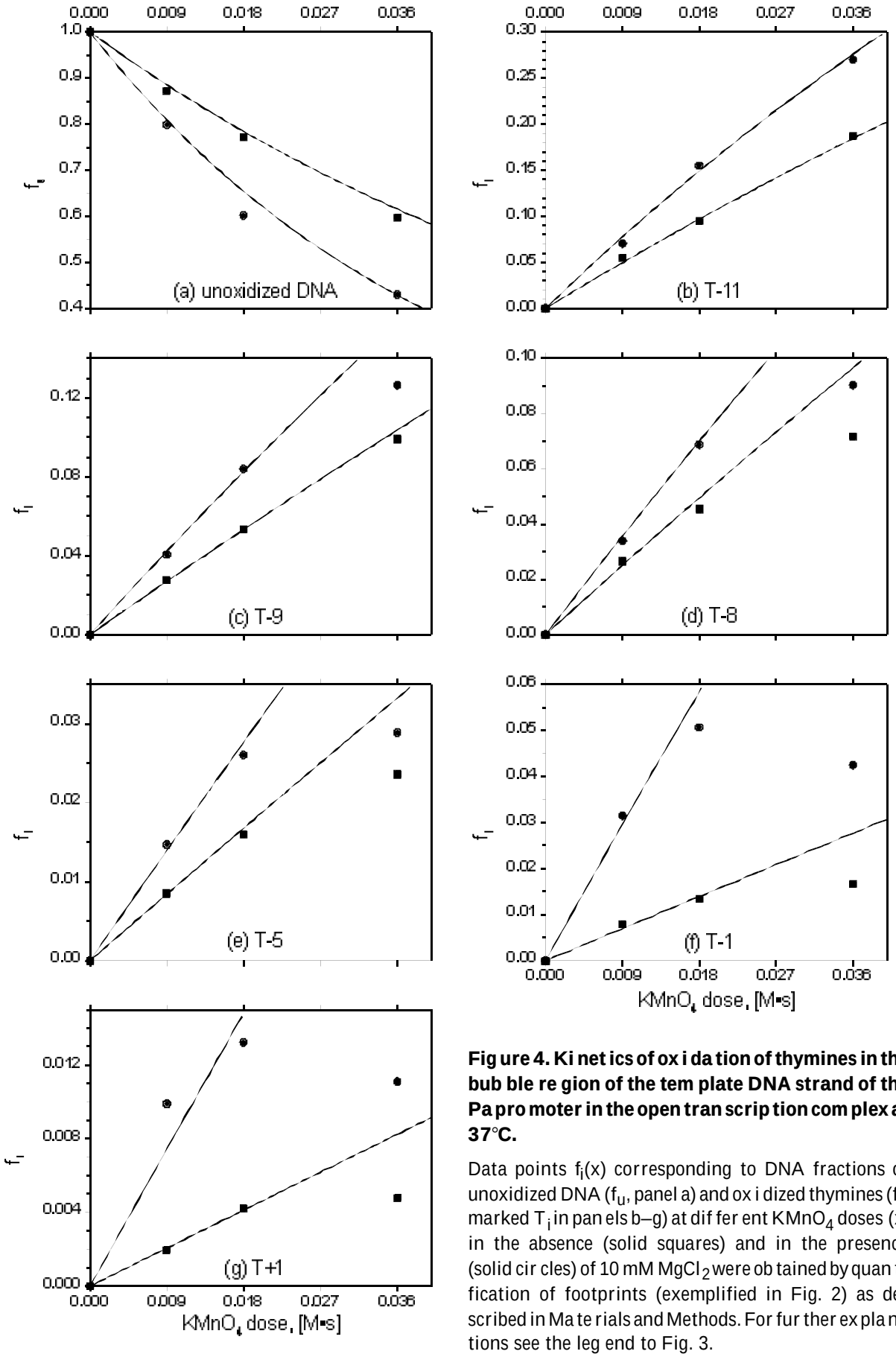

Figure 4. Kinetics of oxidation of thymines in the bubble region of the template DNA strand of the Pa promoter in the open transcription complex at 37°C.

Data points $f_i(x)$ corresponding to DNA fractions of unoxidized DNA (f_u, panel a) and oxidized thymines (f_i, marked T_i in panels b–g) at different $KMnO_4$ doses (x) in the absence (solid squares) and in the presence (solid circles) of 10 mM $MgCl_2$ were obtained by quantification of footprints (exemplified in Fig. 2) as described in Materials and Methods. For further explanations see the legend to Fig. 3.

The approx. 14-bp length of the melted DNA domain in the open complex formed by Eσ^{70} at Pa lies well within the limits of 12–15 bp found to become accessible to footprinting agents in a num ber of other cog nate pro moter complexes thus far studied [15, 35]. The length of the melted DNA re gion is most prob a bly pre de ter mined by lo ca tion of the –10 re gion and the +1 site within the structure of Eσ^{70} [9, 36–39]. According to the recent model of RP_O [39], based on crys tal struc ture of *T. aquaticus* core RNA poly mer ase at 3.3 Å resolution [9] and over 100 UV-induced crosslins mapped between individual phos phates of lacUV5 pro moter DNA and in di vid ual segments of Eσ^{70} subunits, the extreme downstream end of the transcription bubble including positions +4 to +1 of the **t** strand and position +4 of the **nt** strand, binds deep within the ac tive-center cleft while the re main der of the tran scrip tion bub ble up to po si tion –11 of the **t** strand rises from the floor of the ac tive-center cleft along an axis per pen dic u lar to the he lix axis of the down stream du plex. So the lim its of the bub ble re gion found for RP_O at the Pa pro moter are in agree ment with this model.

The model [39] provides also a structural frame work for in ter pre ta tion of the ob served oxidizability pattern of Ts in both sin gle-stranded DNA strands within the bubble region of the open Eσ^{70}–Pa complex. The **t** strand of the transcription bubble is held within an apparent channel formed by β and β' subunits leading from the extreme down stream end surrounding position +1 at the floor of the active-center cleft, about 20 Å from the ac tive-center Mg^{2+}, to wards the edge of the holoenzyme. This channel is large enough to accomodate the A-form DNA:RNA hybrid formed during ini tial abor tive syn the sis of RNA, so that the reactive 5,6 double bond of all the un paired Ts at and up stream of position +1 should be sterically accessible to MnO_4^- anions (similar in size and shape to ortophosphate). The ap par ent re ac tiv ity of Ts can be ex pected to de pend, how ever, both on

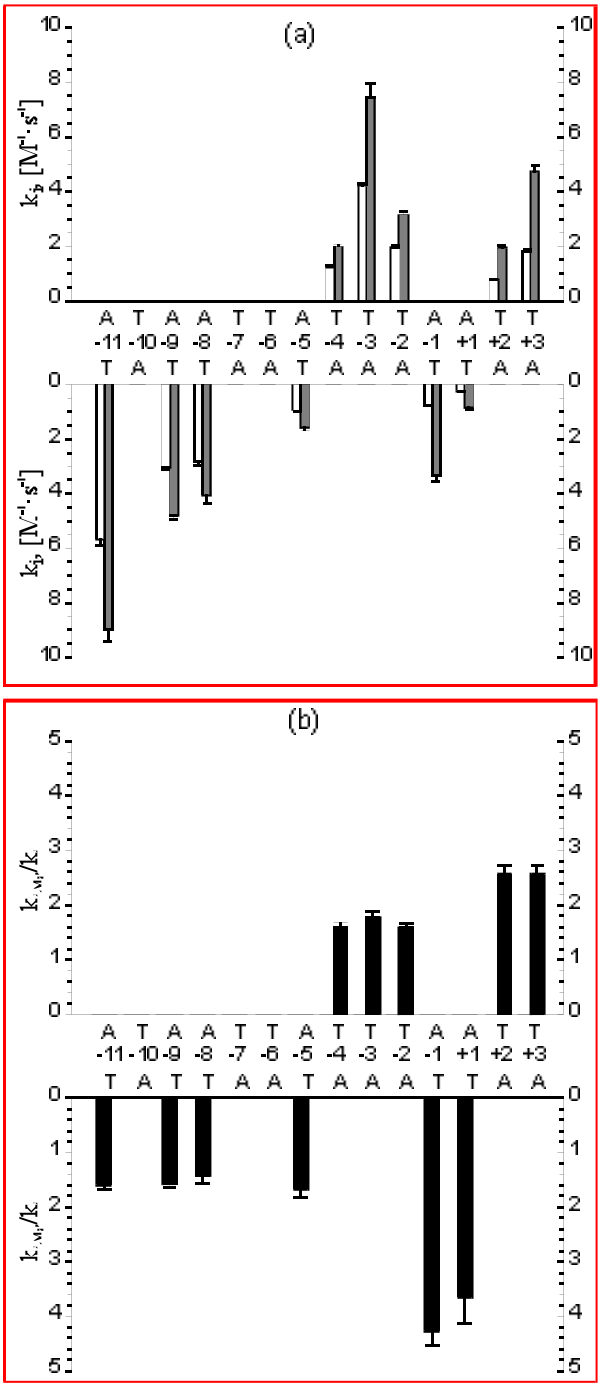

Figure 5. Rate constants of oxidation by $KMnO_4$ of thy mine res i dues in the tran scrip tion bub ble of the open com plex formed at pro moter Pa by *E. coli* RNA poly mer ase.

Panel (a): white and gray col umns cor re spond to k_i de ter mined in the ab sence of Mg^{2+} and in the pres ence of 10 mM $MgCl_2$, re spec tively; panel (b): plot of $k_{i,Mg}/k_i$ ra tios. Sequence above the nu mer i cal scale, in di cat ing positions of the bases in Pa promoter DNA, cor re sponds to the nontemplate strand, se quence be low this scale – to the tem plate strand.

sterical and electrostatic accessibility of MnO_4^- anions to the reaction center. The low reactivity of Ts at or close to the +1 promoter region, being fully accessible to specific base-pairing with initiating NTPs, together with its marked enhancement in the presence of Mg^{2+} strongly suggest that kinetics of oxidation of these bases is primarily under the control of a high electrostatic barrier. Binding sites for Mg^{2+} within the active-center of RP_O are most likely aspartates in the conserved motif NADFDGD of the β' subunit [8, 36]. They were implicated in chelating catalytically active Mg^{2+} ions [8] since their replacement by Fe^{2+} in the open complex of $E\sigma^{70}$ at T7A1 promoter led to cleavage of the template DNA strand around +1 position in the Fenton reaction, whereas $E\sigma^{70}$ carrying the triple D → A mutant in the NADFDGD motif failed to cleave this DNA strand in the presence of Fe^{2+}. Inspection of the footprints of RP_O formed at the A1T7 promoter by the mutant $E\sigma^{70}$ lacking the specific binding sites for Mg^{2+} in the catalytic center (cf. Fig. 3 of ref. [8]) shows that in the presence of 10 mM $MgCl_2$ some thymines close to +1 position were weakly oxidized. The anionic binding sites in this region of the latter complex screened by Mg^{2+} are, of course, DNA phosphates. The increased reactivity of T residues located in **t** strand close to the catalytic center of RP_O formed by wild $E\sigma^{70}$ can thus be explained reasonably by electrostatic shielding by Mg^{2+} ions of negative charges of aspartates of the NADFDGD motif and of ssDNA phosphates.

The observation that the triple D → A mutant in the NADFDGD motif of $E\sigma^{70}$ is able to form RP_O in the absence of Mg^{2+} [8] supports our conclusion that these ions are not required for the open complex formation by wild $E\sigma^{70}$ at the Pa. Recent stopped-flow spectrofluorometric investigations on the kinetics of open complex formation have also indicated that DNA opening is not affected by Mg^{2+} ions [40].

The gradually increasing reactivity of Ts in the **t** strand with their distance from the +1 promoter site, together with the uniform and smaller effect of Mg^{2+} ($k_{i,Mg}/k_i \cong 1.6$) for T–5, T–8, T–9 and T–11, suggest that the observed variation in k_i may be due to a parallel decrease of the sterical barrier for the oxidation towards the edge of the **t**-strand channel, at a constant height of the electrostatic barrier associated with ssDNA phosphates.

The nontemplate strand along the entire length of the bubble domain of RP_O, upstream the tightly constrained extreme downstream end within the active-center cleft (see infra), lies in a deep narrow groove the walls of which are made by a fragment of the β subunit, and in the –10 region contacts σ^{70} region 2 "capping" DNA in the active-center cleft [39]. There are several lines of evidence that strongly conserved **nt** strand adenines: –11, –9 and –8 are involved in specific interactions with residues Y425, Y430, W433 and W434 in the sequence YKFSTYATWW of the conserved subregion 2.3 of σ^{70} forming the ssDNA binding site on the pathway to RP_O formation and play an important role in the nucleation and maintenance of promoter melting [35, 39, 41]. All these residues are aligned along one face of the amphipatic helix 14 in the crystal structure of σ_2^{70} [42] which contains also Q437 implicated in recognition of the conserved –12 A–T base pair, unmelted in most promoters. The very low if any oxidizability of T residues in the –10 region of RP_O at the Pa promoter: T–10 and T–7 and T–6 of the **nt** strand of promoter Pa, can be thus explained by their sterical inaccessibility to MnO_4^-. Relatively high reactivity of T–4, T–3 and T–2 (cf. Fig. 5) indicates that these bases are similarly accessible to the oxidant as the distantly located Ts in the **t** strand and thus are probably not involved in specific interactions with amino acid side chains of $E\sigma^{70}$ domains in contact with DNA backbone phosphates. The magnitude of the Mg^{2+} effect for these bases, $k_{i,Mg}/k_i \cong 1.6$, is the same as for

their distantly located counterparts in the **t** strand; this indicates that the electrostatic barrier to oxidation is also associated with negative charges of ssDNA phosphates. It is apparent from the RP_O model [39] that thymines T+2 and T+3 are located further apart from the Mg^{2+} locus within the active-center than T+1 and T–1 of the **t** strand. This explains why the magnitude of the Mg^{2+} effect for these bases, $k_{i,Mg}/k_i \cong 2.6$, is distinctly smaller than for those in the **t** strand.

Reactivity of sterically accessible Ts depends on local effective concentration of MnO_4^-, which in turn depends on the extent of condensation of counterions on negatively charged DNA phosphates. Preferential diffusive condensation of Mg^{2+} at 10 mM concentration in the presence of 100 mM monovalent electrolyte [43] lowers the height of a negative electrostatic barrier making thus thymine residues apparently more reactive towards the oxidant.

Our preliminary footprinting experiments aimed at determination of k_i in function of Mg^{2+} concentration indicate that the two classes of Mg-binding sites, aspartates and phosphates, differ in the magnitude of the respective dissociation constant, K_d, being about 3-fold smaller for aspartates within the catalytic center of the open complex. Thus, the different magnitude of the effect of Mg^{2+} observed for the two groups of Ts seems to be due primarily to different occupancy of binding sites at a given $MgCl_2$ concentration.

The interpretation of the effect of Mg^{2+} ions on the reactivity of thymine residues outside the catalytic center of the open complex in terms of electrostatic interactions is strongly supported by the results of our parallel studies on their effect on permanganate oxidiation of pyrimidines in double-stranded pDS3 plasmid DNA [27]. Reaction rate constants of oxidation of the majority of pyrimidines of the Pa promoter in the double-stranded DNA form, were generally 2–3 orders of magnitude lower than those measured for the same Ts in the single-stranded DNA domain of the open complex, while in the presence of 10 mM Mg^{2+} were found larger by a factor varying in the range of 2–3 in a sequence-dependent way. A similar effect of Mg^{2+} on oxidizability of pyrimidines in free dsDNA and within the open transcription complex in ssDNA embedded in protein matrix [39] strongly suggests that in both cases the main underlying mechanism of the enhancement of reactivity of thymines towards MnO_4^- anions is the electrostatic shielding of negative charges of phosphates by counterions condensed on DNA surface.

The reduction by bound Mg^{2+} of negative charge density due to the $E\sigma^{70}$ carboxylates and DNA phosphates, leading to an increase in local concentrations of MnO_4^- and $Fe(EDTA)^{2-}$ anions, has been proposed previously [12] as a possible explanation of the increased reactivity of DNA bases and backbone close the start site of λP_R promoter in RP_O. A similar, though smaller, effect of Mg^{2+} on modification of thymines by the highly polarized hexacoordinate OsO_4–2,2'-bipyridine complex [13, 41] in our opinion can be analogously rationalized. In view of the multistep mechanizm of thymine glycol formation in the latter reaction [44], the effect of Mg^{2+} on the reactivity of Ts is probably more complex.

The claimed smaller length of this region in the open complex formed at the λP_R promoter in the absence of $MgCl_2$, called RP_{O1}, and its extension to the full 14 bp length in the transcriptionally competent RP_{O2} form upon binding of Mg^{2+} [11] can be due to insufficient sensitivity of detection of weakly oxidizable Tresidues located close to the +1 position on either DNA strand at the selected single oxidant dose, as they come up more clearly in footprints only in the presence of bound Mg^{2+} ions. Similar remark seems to apply to "Mg-induced extension" of T7A1 promoter [13] probed by OsO_4–2,2'-bipyridine at a very low level of DNA oxidation (estimated as ≤ 10%); under these conditions DNA bands due

to T+1 and T+2 might have not appeared in the absence of Mg^{2+} owing to the very low reactivity of the two bases.

CONCLUDING REMARKS

The presented analysis of kinetics of oxidation by $KMnO_4$ of thymine residues under controlled single-hit conditions in the open promoter complex formed by *E. coli* RNA polymerase at the Pa promoter has unequivocally demonstrated that binding of Mg^{2+} ions does not influence the length of the melted DNA region. In the light of the most recent structural model of RP_O [39], formation of the open complexes at other cognate promoters may appear also to be independent of Mg^{2+}, because the upper length of the melted DNA region seems to be predetermined by the structure of $E\sigma^{70}$. The obtained distribution pattern of the oxidation rate constants of thymines within the transcription bubble provides a measure of their relative sterical accessibility within each of ssDNA strands in the open complex structure.

Earlier claims that binding of Mg^{2+} ions to the open complex is required for extension of the melted DNA region to its full length, from the nucleation site around –10 position downstream to the region of the transcription start-point, were based on the single-dose footprinting experiments. In such experiments, if the oxidant dose is too low, oxidation of weakly reactive pyrimidine residues around the +1 region can easily be overlooked. The extent of the promoter DNA melting can be, of course, affected by sequence-dependent thermodynamic stability of the bubble region and thus also by temperature at which a footprinting experiment is carried out. A meaningful comparison of the melting properties of open complexes formed at different promoters can be thus made only on the basis of pyrimidine reactivity rate constants towards a given oxidant measured under similar experimental conditions.

REFERENCES

1. Springgate, C.F. & Loeb, L.A. (1975) On the fidelity of transcription by *Escherichia coli* ribonucleic acid polymerase. *J. Mol. Biol.* **97**, 577–591.
2. Krakow, J.S., Rhodes, G. & Jovin, T.M. (1976) RNA polymerase: Catalytic mechanisms and inhibitors; in *RNA Polymerase* (Losick, R. & Chamberlin, M., eds.) pp. 127–157, Cold Spring Harbor Laboratory Press, New York.
3. Wu, C.-W. & Goldthwait, D.A. (1969) Studies on nucleotide binding to the ribonucleic acid polymerase by a fluorescence technique. *Biochemistry* **8**, 4450–4458.
4. Koren, R. & Mildwan, A.S. (1977) Magnetic resonance and kinetic studies of the role of divalent cation activator of RNA polymerase from *Escherichia coli. Biochemistry* **16**, 241–249.
5. Burgess, P.M.J. & Eckstein, J. (1978) Absolute configuration of diastereoisomers of adenosine 5′-*O*-(1-thio-triphosphate); Consequences for the stereochemistry of polymerization by DNA-dependent RNA polymerase from *Escherichia coli. Proc. Natl Acad. Sci. U.S.A.* **75**, 4798–4800.
6. Szafrañski, P., Smagowicz, W.J. & Wierzchowski, K.L. (1985) Substrate selection by RNA polymerase from *E. coli.* The role of ribose and 5′-triphosphate fragments and nucleotides interaction. *Acta Biochim. Polon.* **32**, 329–349.
7. Sousa, R., Chung, Y.J., Rose, J.P. & Wang, B.-C. (1993) Crystal structure of bacteriophage T7 RNA polymerase at 3.3Å resolution. *Nature* **364**, 593–599.
8. Zaychikov, E., Martin, E., Denissova, L., Kozlov, M., Markovtsov, V., Kashlev, M., Heumann, H., Nikiforov, V., Goldfarb, A. & Mustaev, A. (1996) Mapping of catalytic residues in the RNA polymerase active center. *Science* **273**, 107–109.

9. Zhang, G., Campbell, E., Minakhin, L., Richter, C., Severinov, K. & Darst, S. (1999) Crystal structure of *Thermus aquaticus* core RNA polymerase at 3.3 Å resolution. *Cell* **98**, 811–824.

10. Suh, W.-C., Leirmo, S. & Record, Jr., M.T. (1992) Roles of Mg^{2+} in the mechanism of formation and dissociation of open complexes between *Escherichia coli* RNA polymerase and the λP_R promoter: Kinetic evidence for a second open complex requiring Mg^{2+}. *Biochemistry* **31**, 7815–7825.

11. Suh, W.-C., Ross, W. & Record, Jr., M.T. (1993) Two open complexes and a requirement for Mg^{2+} to open the λP_R transcription start site. *Science* **259**, 358–361.

12. Craig, M.L., Suh, W.-C. & Record, Jr., M.T. (1995) $HO^{\bullet}$ and DNase I probing of $E\sigma^{70}$ RNA polymerase-λP_R promoter open complexes: Mg^{+2} binding and its structural consequences at the transcription start site. *Biochemistry* **34**, 15624–15632.

13. Zaychikov, E., Denissova, L., Meier, T., Gotte, M. & Heumann, H. (1997) Influence of Mg^{2+} and temperature on formation of the transcription bubble. *J. Biol. Chem.* **272**, 2259–2267.

14. deHaseth, P.L. & Helmann, J.D. (1995) Open complex formation by *Escherichia coli* RNA polymerase: The mechanism of polymerase-induced strand separation of double helical DNA. *MicroReview Mol. Microbiol.* **16**, 817–824.

15. deHaseth, P.L., Zupancic, M.L. & Record, Jr., M.T. (1998) RNA polymerase-promoter interactions: The comings and goings of RNA polymerase. *J. Bacteriol.* **180**, 3019–3025.

16. Chen, Y.-F. & Helmann, J.D. (1997) DNA-melting at the *Bacillus subtilis* flagellin promoter nucleates near –10 and expands unidirectionally. *J. Mol. Biol.* **267**, 47–59.

17. Meier, T., Schickor, P., Wedel, A., Cellai, L. & Heumann, H. (1995) *In vitro* transcription close to the melting point of DNA: Analysis of *Thermatoga maritima* RNA polymerase-promoter complexes at 75°C using chemical probes. *Nucleic Acids Res.* **23**, 988–994.

18. Tsodikov, O.V., Craig, M.L., Saecker, R.M. & Record, Jr., M.T. (1998) Quantitative analysis of multiple-hit footprinting studies to characterize DNA conformation changes in protein–DNA complexes; Application to DNA opening by $E\sigma^{70}$ RNA polymerase. *J. Mol. Biol.* **283**, 757–769.

19. £oziński, T., Markiewicz, W.T., Wyrzykiewicz, T.K. & Wierzchowski, K.L. (1989) Effect of the sequence-dependent structure of the 17 bp AT spacer on the strength of consensus-like *E. coli* promoters *in vivo*. *Nucleic Acids Res.* **17**, 3855–3863.

20. £oziński, T., Adrych-Rozek, K., Markiewicz, W.T. & Wierzchowski, K.L. (1991) Effect of DNA bending in various regions of a consensus-like *Escherichia coli* promoter on its strength *in vivo* and structure of the open complex *in vitro*. *Nucleic Acids Res.* **19**, 2947–2953.

21. £oziński, T. & Wierzchowski, K.L. (1996) Effect of reversed orientation and length of A_nT_n DNA bending sequences in the –35 and spacer domains of a consensus-like *Escherichia coli* promoter on its strength *in vivo* and gross structure of the open complex *in vitro*. *Acta Biochim. Polon.* **43**, 265–280.

22. Kolasa, I. (2001) *Effect of $A_n \cdot T_n$ DNA bending tracts on kinetics of transcription initiation in vitro*. Ph.D. Thesis, Institute of Biochemistry and Biophysics, Polish Academy of Sciences, Warszawa (in Polish).

23. Roe, J.-H., Burgess, R.R. & Record, Jr., M.T. (1984) Kinetics and mechanism of the interaction of *Escherichia coli* RNA polymerase with the λP_R promoter. *J. Mol. Biol.* **176**, 495–521.

24. Roe, J.-H., Burgess, R.R. & Record, Jr., M.T. (1985) Temperature dependence of the rate constants of the *Escherichia coli* RNA polymer-

ase–λP_R promoter interaction. Assignment of the kinetic steps corresponding to protein conformational change and DNA opening. *J. Mol. Biol.* **184**, 441–453.

25. Buc, H. & McClure, W.R. (1985) Kinetics of open complex formation between *Escherichia coli* RNA polymerase and lacUV5 promoter. *Biochemistry* **24**, 2712–2723.

26. Duval-Valentin, G. & Ehrlich, R. (1987) Dynamic and structural characterization of multiple steps during complex formation between *E. coli* RNA polymerase and the tetR promoter from pSC101. *Nucleic Acids Res.* **15**, 575–594.

27. Łoziński, T. & Wierzchowski, K.L. (2001) Effect of Mg^{2+} on kinetics of oxidation of pyrimidines in duplex DNA by potassium permanganate. *Acta Biochim. Polon.* **48**, 511–523.

28. Burgess, R.R. & Jendrisak, J.J. (1975) A procedure for the rapid, large-scale purification of *Escherichia coli* DNA-dependent RNA polymerase involving polymin P precipitation and DNA-cellulose chromatography. *Biochemistry* **14**, 4634–4638.

29. Sternbach, H., Engelhardt, R. & Lesius, A.G. (1975) Rapid isolation of highly active RNA polymerase from *Escherichia coli* and its subunits by matrix-bound heparin. *Eur. J. Biochem.* **60**, 51–55.

30. Sasse-Dwight, S. & Gralla, J.D. (1989) $KMnO_4$ as a probe for lac promoter DNA melting and mechanism *in vivo*. *J. Biol. Chem.* **264**, 8074–8081.

31. Sasse-Dwight, S. & Gralla, J.D. (1991) Footprinting protein–DNA complexes *in vivo*. *Methods Enzymol.* **208**, 146–168.

32. Hayatsu, H. & Ukita, H. (1967) The selective degradation of pyrimidines in nucleic acids by permanganate oxidation. *Biochem. Biophys. Res. Commun.* **29**, 556–561.

33. Borowiec, A., Zhang, L., Sasse-Dwight, S. & Gralla, J.D. (1987) DNA supercoiling promotes formation of a bent repression loop in lac DNA. *J. Mol. Biol*. **196**, 101–111.

34. Ide, H., Kow, Y.W. & Wallace, S.S. (1985) Thymine glycols and urea residues in M13 DNA constitute replicative blocks *in vitro*. *Nucleic Acids Res.* **13**, 8035–8052.

35. Helmann, J.D. & deHaseth, P.L. (1999) Protein–nucleic acid interactions during open complex formation investigated by systematic alternation of the protein and DNA binding partners. *Biochemistry* **38**, 5959–5967.

36. Mustaev, A., Kozlov, M., Markovtsov, V., Zaychikov, E., Denissova, L. & Goldfarb, A. (1997) Modular organization of the catalytic center of RNA polymerase. *Proc. Natl. Acad. Sci. U.S.A.* **94**, 6641–6645.

37. Darst, S.A., Polyakov, A., Richter, C. & Zhang, G. (1998) Structural studies of *Escherichia coli* RNA polymerase; in *Mechanisms of Transcription. Cold Spring Harbor Symposia on Quantitative Biology* (Stillman, B., ed.) vol. 63, pp. 269–276, Cold Spring Laboratory Press, Cold Spring Harbor, New York.

38. Finn, R.D., Orlova, E.V., Gowen, B., Buck, M. & van Heel, M. (2000) *Escherichia coli* RNA polymerase core and holoenzyme structures. *EMBO J.* **19**, 6833–6844.

39. Naryshkin, N., Revyakin, A., Kim, Y., Mekler, V. & Ebright, R. (2000) Structural organization of the RNA polymerase-promoter open complex. *Cell* **101**, 601–611.

40. Strainic, Jr., M.G., Sullivan, J.J., Velevis, A. & deHaseth, P.L. (1998) Promoter recognition by *Escherichia coli* RNA polymerase: Effects of the UP element on open complex formation and promoter clearance. *Biochemistry* **37**, 18074–18080.

41. Juang, Y.-L. & Helmann, J.D. (1994) A promoter melting region in the primary sigma factor of *Bacillus subtilis*. Identification of functionally important aromatic amino acids. *J. Mol. Biol*. **235**, 1470–1488.

42. Malhotra, A., Severinova, E. & Darst, S.A. (1996) Crystal structure of a σ^{70} subunit fragment from *E. coli* RNA polymerase. *Cell* **87**, 127–136.

43. Misra, V.K. & Draper, D.E. (1999) The interpretation of Mg^{2+} binding isotherms for nucleic acids using Poisson-Boltzman theory. *J. Mol. Biol.* **294**, 1135–1147.

44. Paleèek, E. (1992) Probing DNA structure with osmium tetraoxide complexes *in vitro*. *Methods Enzymol.* **212**, 139–155.